

# A W-band Self-Injection-Locked Vital Sign Radar Sensor with On-Chip SIW Monopole Antenna in 0.1- $\mu\text{m}$ GaAs pHEMT

Donglin Gao<sup>#</sup>, Shuping Li<sup>#</sup>, Austin Ying-Kuang Chen<sup>\*</sup>, Chung-Tse Michael Wu<sup>#</sup>

<sup>#</sup>Department of Electrical and Computer Engineering, Rutgers University, USA

<sup>\*</sup>Department of Electrical and Computer Engineering, California State University, USA

**Abstract**— This paper presents a highly sensitive and low-power W-band (75-110 GHz) vital sign radar sensor with an integrated monopole antenna using a 0.1- $\mu\text{m}$  GaAs pHEMT technology. The proposed self-injection-locked (SIL) radar sensor consists of an 85.09-GHz single-transistor oscillator, a 4-dB directional coupler, and a -6.7-dBi substrate-integrated-waveguide (SIW) monopole antenna while consuming only 56 mW from a 2-V supply. The frequency-modulated signal at millimeter-wave frequency is extracted using the directional coupler and downconverted via an external harmonic mixer to the baseband (1 MHz) for subsequent signal processing and data acquisition. To estimate the detected vital sign signal, a two-step Fourier analysis technique based on non-overlapped Short-Time Fourier Transform (STFT) and Fast Fourier Transform (FFT) is adopted. The experimental results show that the proposed SIL radar sensor can accurately detect vital signs at a distance up to 0.9 m while achieving an excellent agreement with the ground truth.

**Keywords**—GaAs pHEMT, self-injection-locked (SIL) radar, substrate-integrated-waveguide (SIW), vital sign detection, W-band.

## I. INTRODUCTION

Radar sensors, as one of the potential technologies for biomedical diagnostic and therapeutic applications, have been developed extensively in the past decades. Compared with contact sensors such as electrodes and wearable devices, the use of non-contact and non-invasive radar sensors allows for the remote acquisition of vital sign signals with minimal discomfort [1]. Among various radar sensors developed, such as homodyne or heterodyne Doppler and FMCW radar [2]-[3], the self-injection-locked (SIL) radar, with excellent sensitivity, clutter-immune capability, and low system complexity, has enabled a new way for vital sign detection over the past decade [4]-[8].

With smaller wavelengths of the millimeter-wave (mm-wave) spectrum brought by the fifth generation (5G) FR2 mobile communication, the sensitivity of the radar sensor is increased while the dimension size of the radar system is shrunk, which is suitable to be integrated with other systems. As such, mm-wave radar sensor has been the frontiers of research for healthcare applications in the microwave community [9]-[11].

In this paper, a W-band GaAs SIL radar system is proposed to detect vital sign signals of a human target with low power consumption, as shown in Fig. 1. A substrate-integrated-waveguide (SIW)-based electric monopole antenna [12] operating in  $\text{TE}_{101}$  mode is employed to transmit and receive the mm-wave signal modulated by chest movement of the human target. The received signal will be injected into the GaAs oscillator locking the new oscillation frequency corresponding

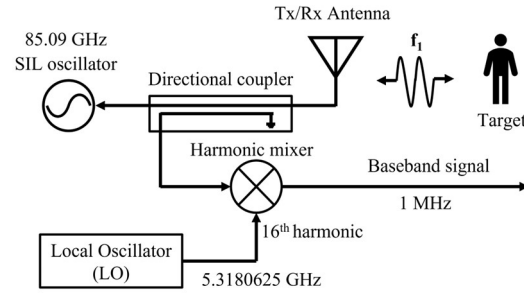


Fig. 1. Block diagram of the proposed GaAs SIL radar system.

to the movement. The frequency-modulated mm-wave signal is extracted using the directional coupler and downconverted to the baseband for subsequent data processing to retrieve the vital sign information. Compared with other W-band doppler radar sensors that requires two separate antennas for transmit and receive [13], the proposed SIL radar can achieve a much smaller form factor using one single built-in on-chip antenna with lower circuit complexity and power consumption. Moreover, instead of using a microwave differentiator topology for signal processing in [5], a two-step Fourier analysis technique using non-overlap short-time Fourier transform (STFT) and Fast Fourier transform (FFT), is applied to estimate the heartbeat and respiration information. To the best of the authors' knowledge, this is the first GaAs SIL radar sensor proposed for non-contact vital sign detection at W-band.

## II. W-BAND SIL RADAR SYSTEM DESIGN

### A. GaAs Radar Circuit Design and On-Chip Antenna

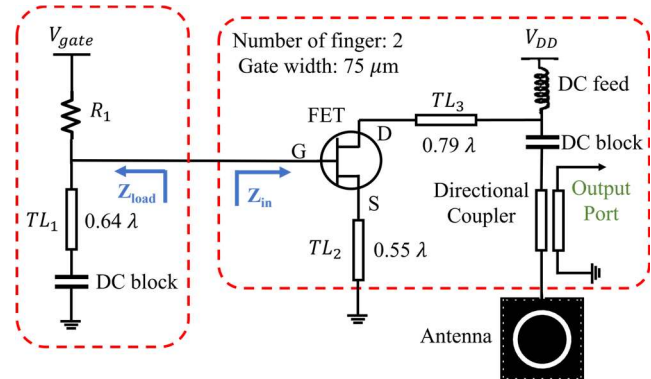


Fig. 2. Schematic of the proposed GaAs SIL radar sensor.

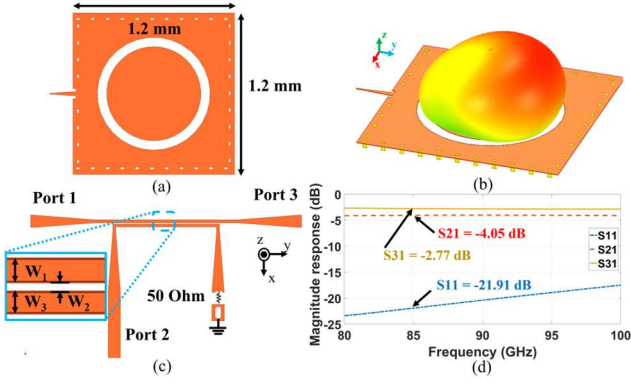


Fig. 3. (a) Top view of the SIW-based monopole antenna, with the size of 1.2 mm  $\times$  1.2 mm. (b) simulated radiation pattern of the SIW-based monopole antenna. (c) topology of the directional coupler, where  $W_1 = W_3 = 7 \mu\text{m}$  and  $W_2 = 3 \mu\text{m}$ . (d) simulated S parameters of the directional coupler.

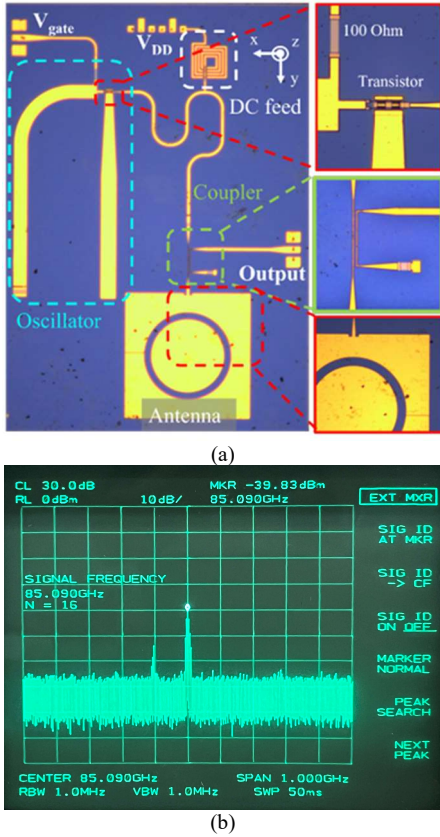


Fig. 4. (a) Chip microphotograph of the SIL radar sensor. (b) output spectrum of the oscillator from spectrum analyzer.

The schematic of the GaAs SIL radar sensor is shown in Fig. 2. The oscillator is designed based on the negative resistance method [14], in which the transistor has two fingers with a gate width of  $75 \mu\text{m}$ . The length and width of  $TL_1$ ,  $TL_2$ , and  $TL_3$  are designed such that the oscillation condition is saturated as  $R_{load} = |R_{in}|/3$  and  $X_{load} = -X_{in}$ , where  $R_{load}$  and  $R_{in}$ ,  $X_{load}$  and  $X_{in}$  are the real and imaginary part of  $Z_{load}$  and  $Z_{in}$ , respectively. When supplied by  $V_{DD}$  and  $V_{gate}$  equal to 2 V and 0 V, respectively, the oscillation is generated at 85.09 GHz, and the power consumption of the oscillator is 56 mW. On the other

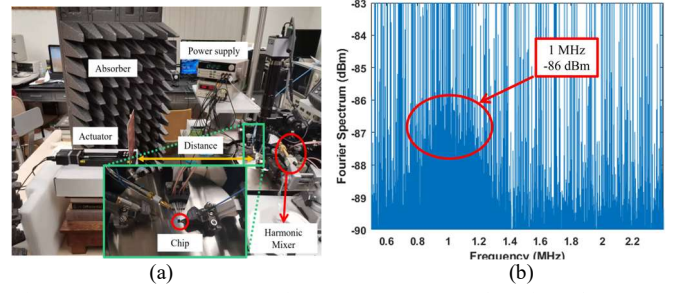


Fig. 5. (a) Measurement setup for actuator movement detection. (b) spectrum of the actuator movement measured at 80 cm.

hand, a SIW-based magnetic-current-loop-induced electrical monopole antenna operating in  $TE_{101}$  mode is utilized for the SIL radar sensor, whose size is 1.2 mm  $\times$  1.2 mm as shown in Fig. 3(a). To facilitate vital sign measurements using the on-chip SIL system on a probe station, the radiation pattern of the antenna at the operating frequency is oriented towards the y-axis, which is the frontal direction of the probe station where the target under test is located. The simulated radiation pattern of the proposed SIW antenna with -6.7 dBi is depicted in Fig. 3(b), which mainly results from the high dielectric constant and thickness of the GaAs substrate. The received signal is directly injected into the oscillator to lock the new oscillation frequency modulated with motion information. The new oscillation frequency is coupled out by a directional coupler shown in Fig. 3(c) and downconverted to the baseband for data processing. The coupler is designed to be  $261 \mu\text{m}$  in length with the transmission line width of  $7 \mu\text{m}$  and spacing of  $3 \mu\text{m}$  between the two coupled lines. The coupling factor of the directional coupler is 4.05 dB, whereas the return loss is 21.91 dB at 85 GHz, and the insertion loss is 2.77 dB, as shown in Fig. 3(d). Fig. 4(a) shows the chip microphotograph of the proposed GaAs SIL radar with the zoom-in view of the transistor, directional coupler, and monopole antenna. The overall chip area is  $12 \text{ mm}^2$ . In addition, the measured oscillation frequency at 85.09 GHz is shown in Fig. 4(b).

#### B. Frequency demodulation and Post Processing

Assuming a human target is located in front of the GaAs SIL radar sensor with the oscillator operating at oscillation frequency ( $\omega_0$ ), the reflected signal modulated by the human movement is injected back into the oscillator to lock the new instantaneous oscillation frequency ( $\omega_1$ ) as:

$$\omega_1 = \omega_0 + \Delta\omega(t) \quad (1)$$

where  $\Delta\omega(t)$  represents the frequency shift corresponding to the target movement. Therefore, the baseband signal down converted from the carrier signal extracted from the directional coupler can be written as:

$$S(t) = A \cos(\omega_1 t) \quad (2)$$

where  $A$  represents the amplitude of the output signal from the coupler. Unlike the topology in [5], where the microwave differentiator is integrated with SIL radar to convert the

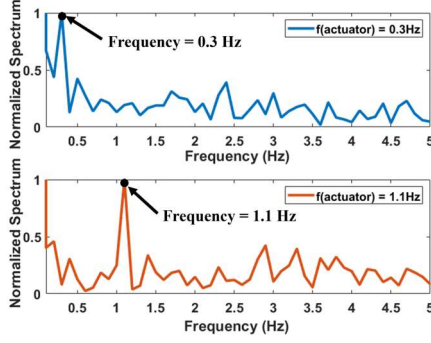


Fig. 6. Frequency spectrum of the downconverted signal.

received signal to the RF signal with corresponding frequency-dependent amplitude variances, a two-step Fourier analysis using the non-overlap STFT and FFT is applied in the post signal processing to extract the vital sign information.

First, Short Time Fourier Transform (STFT) is performed on the acquired baseband signal  $S(t)$  to extract the variation of  $\omega_1$  over time. In this step,  $S(t)$  is divided into multiple non-overlapping small segments containing equal sampling points. Since the acquisition sampling rate of  $S(t)$  is much higher than  $\omega_1$  and the number of sampling points in each segment is sufficiently small,  $\Delta\omega(t)$  can be regarded as constant in each segment and only varies among different segments. Moreover,  $\omega_0$ , which represents the original oscillation frequency remains constant during the acquisition period of  $S(t)$ . Thus,  $\omega_1$  does not change with respect to the time for each small segment. Then  $\omega_1$  of each segment is obtained by applying FFT in each segment. Furthermore, the resulting  $\omega_1$  of each segment is recombined to obtain a piece of data representing variation of the  $\omega_1$  with respect to time.

On the other hand, the changing frequency  $\Delta\omega(t)$  in the time domain can simply be written as [15]:

$$\Delta\omega(t) = B \sin\left(\frac{2\omega_0}{c}d + x_b(t)\right) \quad (3)$$

where  $B$ ,  $c$ , and  $d$  represent the locking range, speed of light, and the initial distance from the target to the SIL radar, respectively.  $x_b(t)$  represents the displacement fluctuation that is caused by the cardiopulmonary motion of the subject, whose variation results in  $\omega_1$  changing over time. Then, the second FFT is performed on the new data generated by STFT, to extract the frequency  $x_b(t)$  which contains a combination of the respiration rate and heartbeat rate of the human target. As a result, by utilizing the two-step FFT processing, the proposed GaAs SIL radar system can be used to estimate the vital sign information of the target.

### III. EXPERIMENTAL RESULT

#### A. Actuator Movement Detection

To demonstrate the feasibility of the proposed SIL radar system, the SIL radar is first utilized to detect the movement of the actuator-mounted metallic plate. The measurement setup is shown in Fig. 5(a). The vibration frequency and displacement

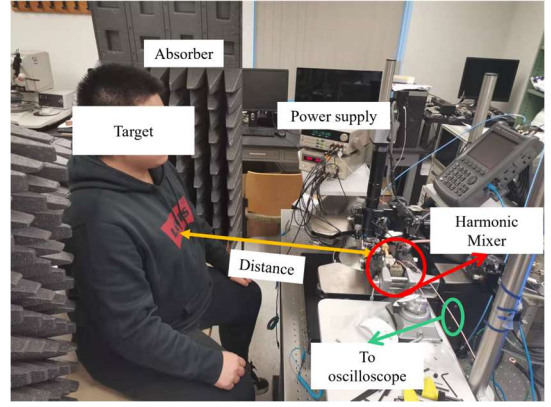


Fig. 7. Human target measurement setup.

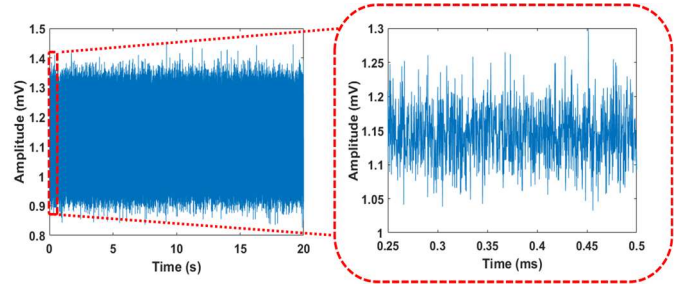


Fig. 8. Time-domain vital sign results of the GaAs SIL radar when  $d = 0.6$  m.

range of the actuator are picked as 0.3 Hz with 2.39 mm and 1.1 Hz with 2.26 mm to simulate the movement of the human chest affected by respiration and heartbeat, respectively. The actuator is placed in the front of the probe station, at a distance of 0.8 m from the proposed SIL radar sensor. The coupled output signal from the oscillator will be transferred to the HP 11970A harmonic mixer and downconverted to 1 MHz mixed by the 16<sup>th</sup> harmonic of the signal generated by HP 8671A signal generator. An R&S RTE1022 oscilloscope is used for data acquisition of the baseband signal and the acquired data will be sent to the laptop for post-processing. The measurement duration for each scenario is 10 seconds with 10 MHz sampling rate. Fig. 5(b) shows the Fourier frequency spectrum of the baseband signal acquired by the oscilloscope, where the downconverted oscillation frequency lies at 1 MHz with the signal output of -86 dBm, which is only 4 dBm larger than the noise signal due to the conversion loss of harmonic mixer, as it is designed to work at Ka-band instead of W-band.

Fig. 6 plots the measurement result, where the peaks of the output spectrum are located at 0.3 Hz and 1.1 Hz corresponding to the vibration of the actuator movement respectively. The result demonstrates the feasibility of the SIL radar sensor and its accuracy in detecting the frequency of target movements.

#### B. Vital Sign Detection

Furthermore, the SIL radar sensor is then used to detect the vital sign signals of the human target. Fig. 7 shows the measurement setup for detecting vital sign signals using the proposed SIL radar. The total measurement duration is 20 secs with 5 MHz sampling rate. Fig. 8 illustrates the time domain



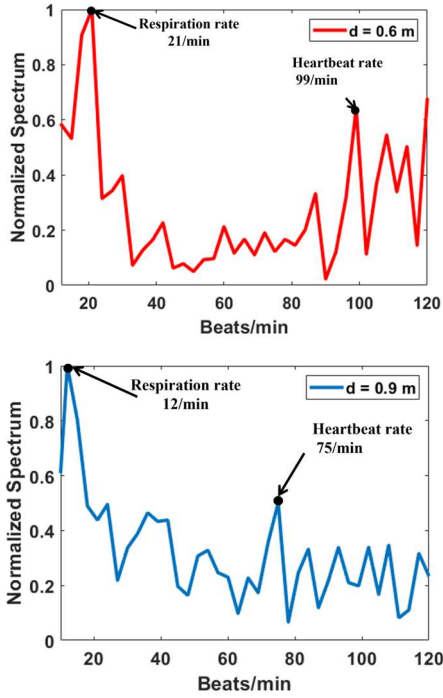


Fig. 9. Extracted vital sign results from the GaAs SIL radar when  $d = 0.6$  m and  $d = 0.9$  m.

Table 1. Comparison of the estimated vital sign with ground truth at the distance of  $d = 0.6$  m and  $d = 0.9$  m.

Distance (m)	0.6	0.9
<b>Respiration Rate (Beats/min)</b>	21	12
<b>Ground Truth</b>	24	12
<b>Heartbeat Rate (Beats/min)</b>	99	75
<b>Ground Truth</b>	99	78

vital sign results of the on-chip SIL radar system when the target is located at the distance of  $d = 0.6$  m. The measured vital sign results of human target located at 0.6 m and 0.9 m are depicted in Fig. 9, respectively. Due to the random body movement of the human target, the Fourier spectrum acquired by the GaAs SIL radar is not as clean as the ones of the sinusoidal movement actuator as shown in Fig. 6. Although the phase pattern of the heartbeat might be distorted by the harmonic of the breathing, both the inspiration and heartbeat rate are obvious and readable in the spectrums. To validate the accuracy, the heartbeat rate acquired by a finger pulse oximeter is counted as the ground truth of the measurement. Table 1 compares the respiration and heartbeat rates using the SIL at the distance of  $d = 0.6$  m and  $d = 0.9$  m. For both distances, the measured respiration rate and heartbeat agree well with the ground truth. Meanwhile, the gain of each vital sign overwhelms nearby noises. Therefore, the proposed SIL radar sensor is able to measure vital signals over a 0.9 m distance with validated high accuracy and reduced size compared with SIL working at a lower frequency.

## IV. CONCLUSION

This work presents the first low-power W-band GaAs SIL radar sensor with on-chip SIW monopole antenna for non-contact vital sign detection. Using the proposed architecture and two-step Fourier analysis technique, the heartbeat and respiration rate of the target can be accurately detected and estimated with excellent agreement with the ground truth. By incorporating antenna-on-GaAs, the overall size of this high-precision vital sign radar sensor can potentially be further miniaturized with improved energy efficiency while maintaining the sensitivity and low circuit complexity.

## REFERENCES

- [1] A. Singh, S. U. Rehman, S. Yongchareon and P. H. J. Chong, "Multi-resident non-contact vital sign monitoring using radar: a review," *IEEE Sens. J.*, vol. 21, no. 4, pp. 4061-4084, Feb. 2021.
- [2] C. Lu, Y. Yuan, C.-H. Tseng and C.-T. M. Wu, "Multi-target continuous-wave vital sign radar using 24 GHz metamaterial leaky wave antennas," *2019 IEEE MTT-S International Microwave Biomedical Conference (IMBioC)*, Nanjing, China, 2019, pp. 1-4.
- [3] Z. Xu *et al.*, "Simultaneous monitoring of multiple people's vital sign leveraging a single phased-MIMO radar," in *IEEE J. Electromagn. RF Microw. Med.*, vol. 6, no. 3, pp. 311-320, Sept. 2022.
- [4] F.-K. Wang, C.-J. Li, C.-H. Hsiao, T.-S. Horng, J. Lin, K.-C. Peng, J.-K. Jau, J.-Y. Li, and C.-C. Chen, "A novel vital-sign sensor based on a self-injection-locked oscillator," *IEEE Trans. Microw. Theory Techn.*, vol. 58, no. 12, pp. 4112-4120, Dec. 2010.
- [5] Y. Yuan, C. Lu, A. Y.-K. Chen, C.-H. Tseng and C.-T. M. Wu, "Multi-target concurrent vital sign and location detection using metamaterial-integrated self-injection-locked quadrature radar sensor," *IEEE Trans. Microw. Theory Techn.*, vol. 67, no. 12, pp. 5429-5437, Dec. 2019.
- [6] F.-K. Wang *et al.*, "Review of self-injection-locked radar systems for noncontact detection of vital signs," in *IEEE Journal of Electromagnetics, RF and Microwaves in Medicine and Biology*, vol. 4, no. 4, pp. 294-307, Dec. 2020.
- [7] F.-K. Wang and J.-X. Zhong, "Self-Injection-Locked (SIL) radars using frequency modulation (FM) techniques for concurrent range and vital sign monitoring," *2022 IEEE MTT-S International Microwave Biomedical Conference (IMBioC)*, 2022, pp. 54-56.
- [8] C.-H. Tseng, L.-T. Yu, J.-K. Huang, and C.-L. Chang, "A wearable self-injection-locked sensor with active integrated antenna and differentiator based envelope detector for vital-sign detection from chest wall and wrist," *IEEE Trans. Microw. Theory Techn.*, vol. 66, no. 5, pp. 2511-2521, May 2018.
- [9] S. Diebold *et al.*, "W-band MMIC radar modules for remote detection of vital signs," *2012 7th European Microwave Integrated Circuit Conference*, Amsterdam, Netherlands, 2012, pp. 195-198.
- [10] S. Schäfer, A. R. Diewald, D. Schmied and S. Müller, "One-dimensional patch array for microwave-based vital sign monitoring of elderly people," *2018 19th International Radar Symposium (IRS)*, Bonn, Germany, 2018, pp. 1-10.
- [11] F. Michler *et al.*, "A radar-based vital sign sensing system for in-bed monitoring in clinical applications," *2020 German Microwave Conference (GeMiC)*, Cottbus, Germany, 2020, pp. 188-191.
- [12] C.-T. M. Wu and T. Itoh, "An X-band dual-mode antenna using substrate integrated waveguide cavity for simultaneous satellite and terrestrial links," *2014 Asia-Pacific Microwave Conference*, Sendai, Japan, 2014, pp. 726-728.
- [13] H. Kim and J. Jeong, "Non-contact measurement of human respiration and heartbeat using W-band Doppler radar sensor," *Sensors*, vol. 20, no. 18, p. 5209, Sep. 2020.
- [14] G. Gonzalez, *Foundations of Oscillator Circuit Design*, Norwood, MA, USA: Artech House, 2007.
- [15] F.-K. Wang, *et al.*, "Concurrent vital sign and position sensing of multiple individuals using self-injection-locked tags and injection-locked I/Q receivers with arctangent demodulation," *IEEE Trans. Microw. Theory Techn.*, vol. 61, no. 12, pp. 4689-4699, Dec. 2013.